JOURNAL OF MATERIALS SCIENCE 26 (1991) 1588–1600

Phase equilibria in the CaF_2–Al_2O_3–CaO system

A. I. ZAITSEV, N. V. KOROLYOV, B. M. MOGUTNOV*
*I.P. Bardin Central Research Institute of Ferrous Metallurgy and *Laboratory of Thermodynamic Investigations, 9/23 Second Bauman Street, 107005 Moscow, USSR*

Computations of phase equilibria in the CaF_2–Al_2O_3–CaO system have been carried out on the basis of experimentally found thermodynamic properties of all intermediate phases and melts. Coordinates of the phase equilibrium boundaries were determined by solving a system of equations expressing equality of chemical potentials of the components in coexisting phases. The nature and quantity of the coexisting phases were established by a search for the Gibbs energy minimum of the system. All the phases of the CaF_2–Al_2O_3–CaO system were taken into consideration. Calculated phase diagrams of the CaO–CaF_2, CaO–Al_2O_3 and CaF_2–Al_2O_3 binary subsystems are in good agreement with the data available in the literature. Isotherms of the CaF_2–Al_2O_3–CaO system were calculated at 1600, 1650, 1723 and 1773 K. A wide region of liquid separation into two phases is observed in the system. One phase is composed of practically pure CaF_2 with additions of several mol% of CaO and Al_2O_3, and the other consists of 50 to 65 mol% of CaF_2 only. Eleven invariant points of the CaF_2–Al_2O_3–CaO system include seven ternary eutectics, two ternary peritectics and two points of four-phase monotectic transition. The primary fields of crystallization of all the phases are alongated toward the CaF_2 apex, the CaO field being the widest and the $3CaO \cdot Al_2O_3$ field the narrowest. Seven junctions of the CaF_2–Al_2O_3–CaO phase diagram were represented. Computed saturation lines of CaF_2–Al_2O_3–CaO melt with CaO, Al_2O_3, $CaO \cdot 6Al_2O_3$ and $CaO \cdot 2Al_2O_3$, and also the positions of a number of characteristic points, agree well with the experimental data available. The present calculations reveal a number of details and peculiarities of the constitution of the CaF_2–Al_2O_3–CaO phase diagram.

1. Introduction

The CaF_2–Al_2O_3–CaO system is a basic one for slags of the ladle treatment of steel, electrometallurgy and welding fluxes. Data on the equilibrium phase diagram of the system available up to date are highly contradictory [1–20]. According to the opinion of some authors (e.g. [1]) the phase diagram of the CaF_2–Al_2O_3–CaO system will alter as the conditions of existence of CaF_2–Al_2O_3–CaO slags undergo change. There is therefore an important problem of detailed analysis of the phase equilibria in the CaF_2–Al_2O_3–CaO system.

In the present study, calculations of phase equilibria in the CaF_2–Al_2O_3–CaO system have been performed on the base of experimentally found thermodynamic properties of all intermediate phases [21, 22] and melts [23, 24]. Gibbs energies of the phase transitions $G^{L\to s}_{Al_2O_3}$, $G^{L\to s}_{CaO}$ and $G^{L\to\beta}_{CaF_2}$ were chosen from the All-Union databank of thermodynamic values, IVTANTERMO. Coordinates of the phase equilibrium boundaries were determined by solving a system of equations expressing equality of chemical potentials of the components in coexisting phases. In every case all the phases of the CaF_2–Al_2O_3–CaO system were taken into consideration. The nature and quantity of the coexisting phases were established by a search for the Gibbs energy minimum of the system.

2. Results and discussion

2.1. The binary CaF_2–Al_2O_3 subsystem

The results obtained for the binary CaF_2–Al_2O_3 subsystem are given in Fig. 1; for comparison the data of other authors are also represented. The CaF_2–Al_2O_3 system is characterized by a simple eutectic phase diagram. The coordinates of the eutectic point ($T = 1670.2$ K and $X_{Al_2O_3} = 0.03016$) as well as the position of the liquidus line on both CaF_2 and Al_2O_3 sides are in good agreement with recommended values [1, 2]. Attention should be drawn to the S-shaped liquidus line on the alumina side. This points to a trend of CaF_2–Al_2O_3 melts to immiscibility, although in reality the phenomenon does not occur. The positions of the liquidus lines found by Hillert [14] are close to that calculated in the present work. However, Hillert [14] observed the existence of a wide region of immiscibility in CaF_2–Al_2O_3 melts. The latter result contradicts both the present calculations and the detailed investigation of Ries and Schwerdtfeger [3]. According to the latter authors the miscibility gap in the liquid phase of the CaF_2–Al_2O_3–CaO system does not reach the CaF_2–Al_2O_3 binary side. A similar S-shaped liquidus line on the alumina side was also observed by Povolotskii *et al.* [5], but its position was at lower temperatures.

0022–2461/91 $03.00 + .12

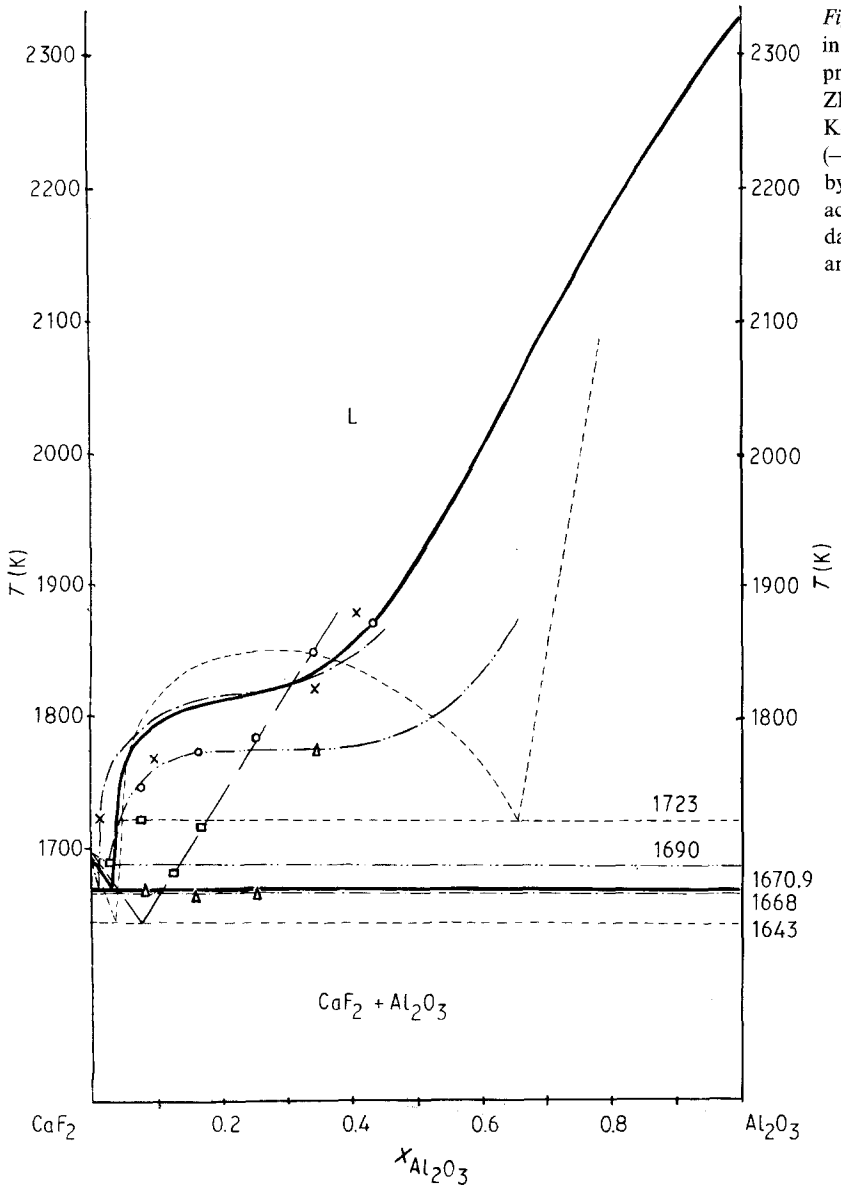

Figure 1 Computed CaF_2–Al_2O_3 phase diagram in comparison with the data available: (——) present calculation; (—·—) recommended by Zhmoidin and Chatterjee [1] and by Mills and Keene [2]; (– – –) recommended by Hillert [14]; (— —) results of Paskal [25]; (—··—) data quoted by Povolotskii *et al.* [5]; (○) $T_{liq.}$ and (△) $T_{sol.}$ according to measurement of Zhmoidin [15]; (□) data of Davies and Wright [16]; (×) data of Ries and Schwerdtfeger [3].

2.2. The binary CaO–Al_2O_3 subsystem

Four intermediate phases CA_6, CA_2, CA and C_3A are formed in CaO–Al_2O_3 system (here and further on $A = Al_2O_3$, $C = CaO$ and $Fl = CaF_2$). In accordance with the present calculations (Fig. 2) all of them decompose before the melting point. In the CaO–Al_2O_3 system there is one deep eutectic point at $T = 1724$ K and $X_{Al_2O_3} = 0.358$. The positions of the characteristic points on the computed phase diagram are in a good agreement with the conclusions of Nurse *et al.* [26], where the experiments were carried out under conditions excluding the penetration of moisture. It was shown by calculations and measurements of the component vapour pressures over appropriate heterogeneous fields of the CaF_2–Al_2O_3–CaO system [21, 22] that the $C_{12}A_7$ compound is not formed in the binary CaO–Al_2O_3 system. It seems to be metastable. This conclusion is confirmed by the results of Kumar and Kay [27] and by data available in the literature (e.g. [1]) which indicate that the $C_{12}A_7$ phase is stabilized by water vapours, gases, fluorides and so on.

2.3. The binary CaF_2–CaO subsystem

The phase diagram of the CaF_2–CaO system (Fig. 3) has been computed previously [28]. It is a simple eutectic diagram with the eutectic point at $T = 1631$ K and $X_{CaO} = 0.198$. The positions of computed liquidus lines in the CaF_2–CaO system agree well with other recommendations [1, 2] and data [3]. In particular, there is good agreement between the results of calculations [28] and direct experimental data on the positions of characteristic points in the same study.

2.4. The ternary CaF_2–Al_2O_3–CaO system

Computed saturation lines of the CaF_2–Al_2O_3–CaO melt with CaO, Al_2O_3, CA_6 and CA_2 at 1873 and 2073 K (Fig. 4) are in good agreement with the results of the latest and most accurate investigation of Ries and Schwerdtfeger [3] as well as with the data of Zhmoidin and Chatterjee [1]. However, the computed position of the immiscibility region in the liquid phase of the CaF_2–Al_2O_3–CaO phase diagram is somewhat different from that suggested in experimental studies [1, 3]. One of the causes of the discrepancy might be connected with the difficulties that are met with in experimental determination of the miscibility gap in liquids that have a tendency to glass formation. It should be noted that the compositions of almost all of the slags used for determination of the region

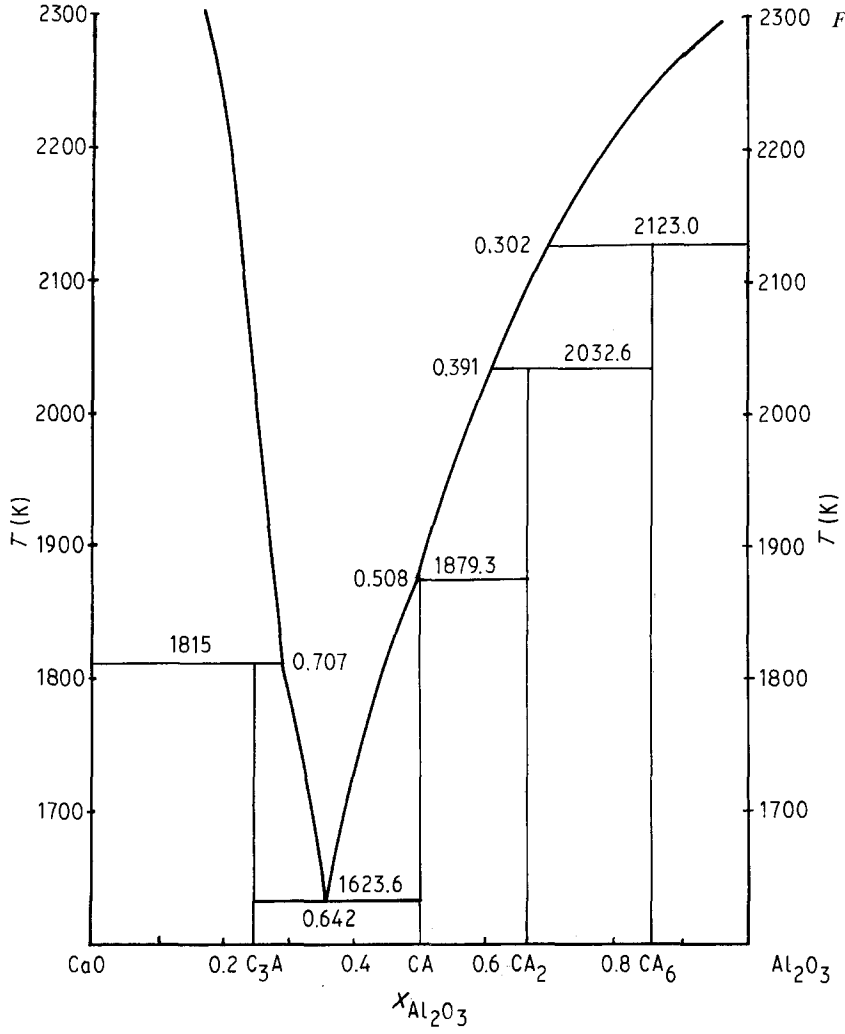

Figure 2 Computed $CaO–Al_2O_3$ phase diagram.

boundaries [1, 3] lie in fact inside the computed immiscibility region. It is therefore possible that chemical analysis of equilibrium quenched slags composed of layers formed by the separation process that are different in content but close in properties might lead to sufficient errors.

Calculated isotherms of the $CaF_2–Al_2O_3–CaO$ system at 1600, 1650, 1723 and 1773 K are shown in Figs 5 to 8. Fig. 9 represents triangulation of the system, designed in accordance with the data [1, 2] and results showing that $C_{12}A_7$ is not formed in the $CaO–Al_2O_3$ system.

There is only a narrow region of liquid phase stability at 1600 K in the $CaO–CaF_2–C_{11}A_7Fl$ triangle (Fig. 5). It is situated around a deeper eutectic with the coordinates; $X_{CaF_2} = 0.378$, $X_{CaO} = 0.464$, $T = 1509$ K. The point of C_3A peritectic formation is situated below the liquid phase region. The other regions characterize equilibria of solid phase that correspond to triangulation.

The region of liquid phase stability is widened significantly at 1650 K (Fig. 6). It occupies part of the $CaF_2–CaO$ binary side and extends into the $CaF_2–C_{11}A_7Fl–C_3A_3Fl$, $CaF_2–C_3A_3Fl–CA_2$ and $CaF_2–CA_2–CA_6$ triangles. A small field of liquid phase stability is also observed in the $C_{11}A_7Fl–CA–C_3A$ triangle around the eutectic of the $CaO–Al_2O_3$ binary subsystem. Immiscibility of the liquid phase does not occur at the temperature mentioned.

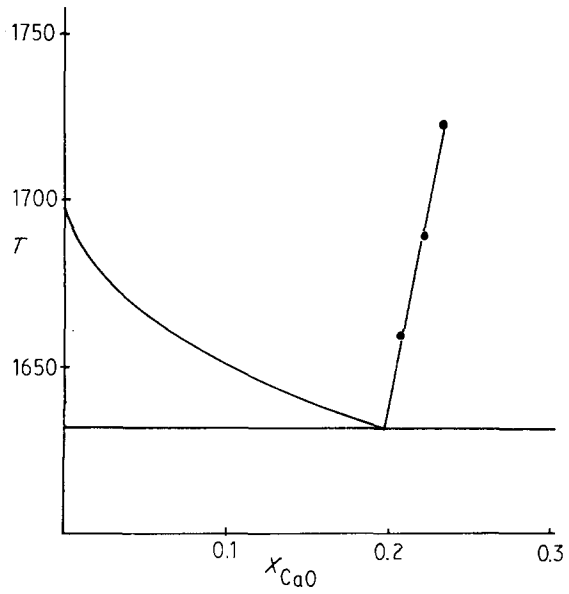

Figure 3 Computed $CaO–CaF_2$ phase diagram. Points designate the position of the liquids line obtained in isothermal evaporation experiments [28].

A wide region of liquid separation into two phases is observed on the isotherm for $T = 1723$ K (Fig. 7), one phase being composed of practically pure CaF_2 with additions of some mol % of CaO and Al_2O_3 and the other consisting of 50 to 65 mol % of CaF_2 only. As the temperature increases to 1773 K (Fig. 8) the

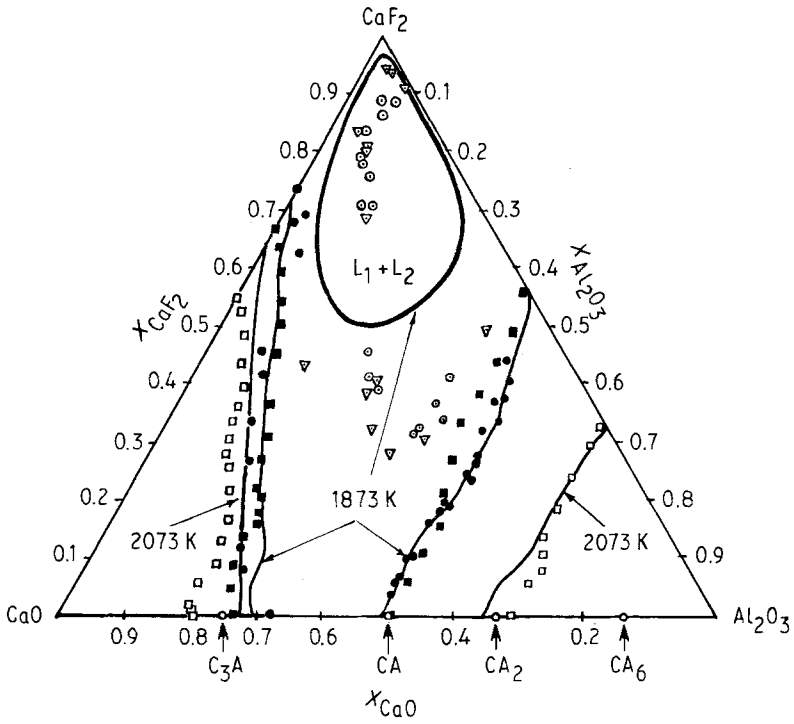

Figure 4 Compositions of CaF_2–Al_2O_3–CaO melts saturated with CaO, Al_2O_3, CA_6 and CA_2 and the miscibility gap. Solid lines represent the present calculations; (□, ■) experimental data reported by Zhmoidin and Chatterjee [1] for $T = 1873$ and 2073 K, respectively; (●) experimental data of Ries and Schwerdtfeger [3] for saturated melts, $T = 1873$ K; (○, ▽) experimental data of Ries and Schwerdtfeger [3] for the miscibility gap boundary, $T = 1873$ K.

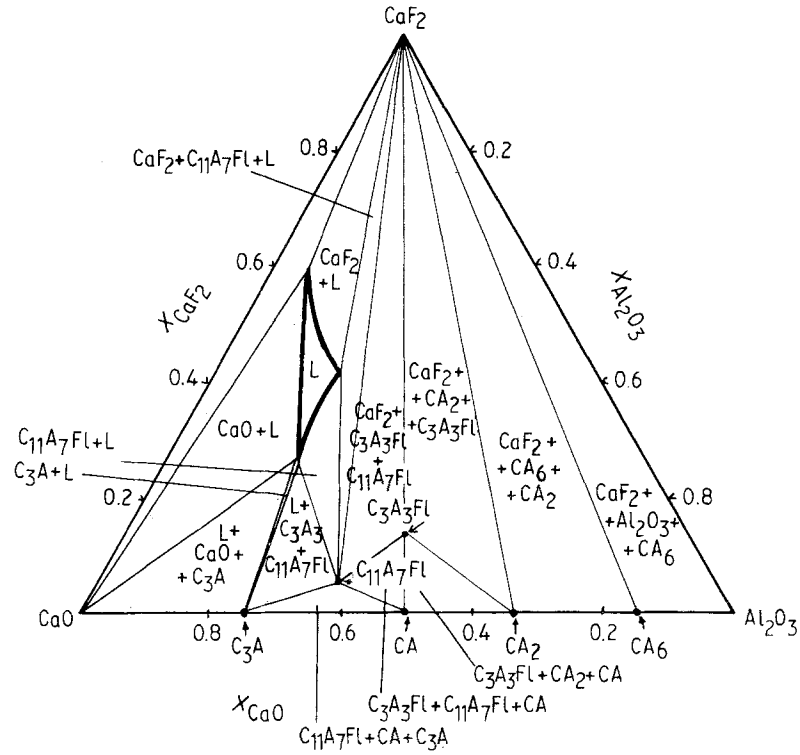

Figure 5 Computed isotherm at $T = 1600$ K for the CaF_2–Al_2O_3–CaO phase diagram.

coordinates of the miscibility gap are practically unchanged. This means that the boundaries of the miscibility gap are practically vertical.

The general characteristics of the CaF_2–Al_2O_3–CaO phase diagram are given in Fig. 10 and Table I, where information about all the invariant points of the system is collected. The slopes of binary crystallization lines are shown in Fig. 10 by arrows. The diagram demonstrates the fields of primary crystallization of CaO, Al_2O_3, CaF_2 and all the binary calcium aluminates. There are two ternary compounds in the system (C_3A_3Fl and $C_{11}A_7Fl$). These have been shown by calculations to melt congruently at 1784 and 1853 K, respectively. The latter result agrees well with the melting points of the compounds determined experimentally (see e.g. [1]): 1780 ± 1.5 K and 1850 ± 2.5 K, respectively.

The primary fields of all the phases are elongated toward the CaF_2 apex, the CaO field being the widest and the C_3A one the narrowest. Eleven invariant points include seven ternary eutectics, two ternary peritectics and two points of four-phase monotectic transition. In Fig. 10 the ternary eutectics are marked with a symbol E and peritectics with P. Point E_1 is a eutectic one for final crystallization of the CA–C_3A_3Fl–CA_2 triangle compositions. The coordinates of E_1 are close to that found by Zhmoidin in experimental investigation [1] (see Table II). It should

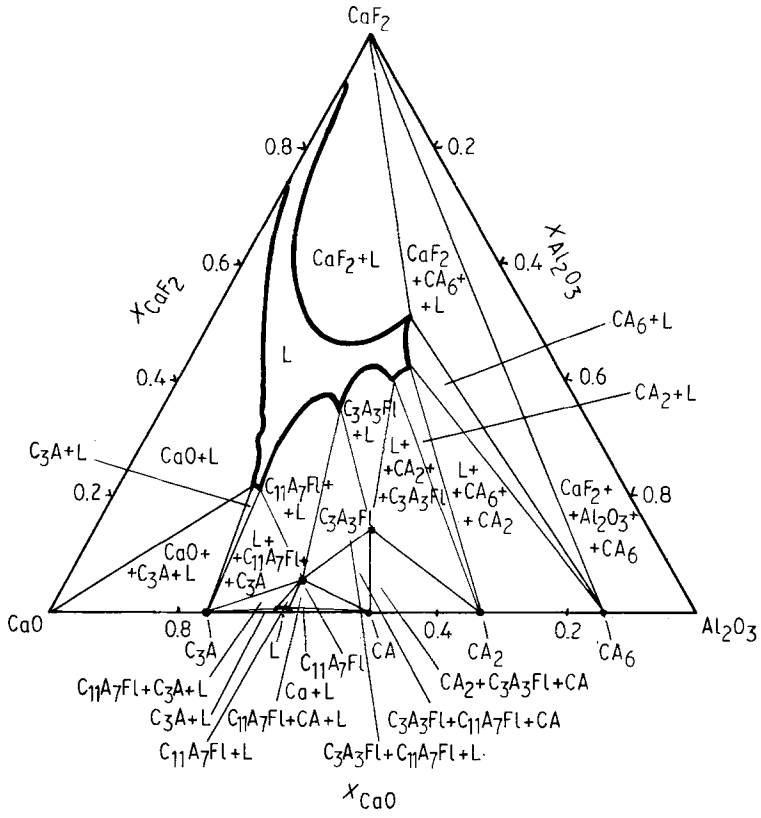

Figure 6 Computed isotherm at $T = 1650$ K for the CaF_2–Al_2O_3–CaO phase diagram.

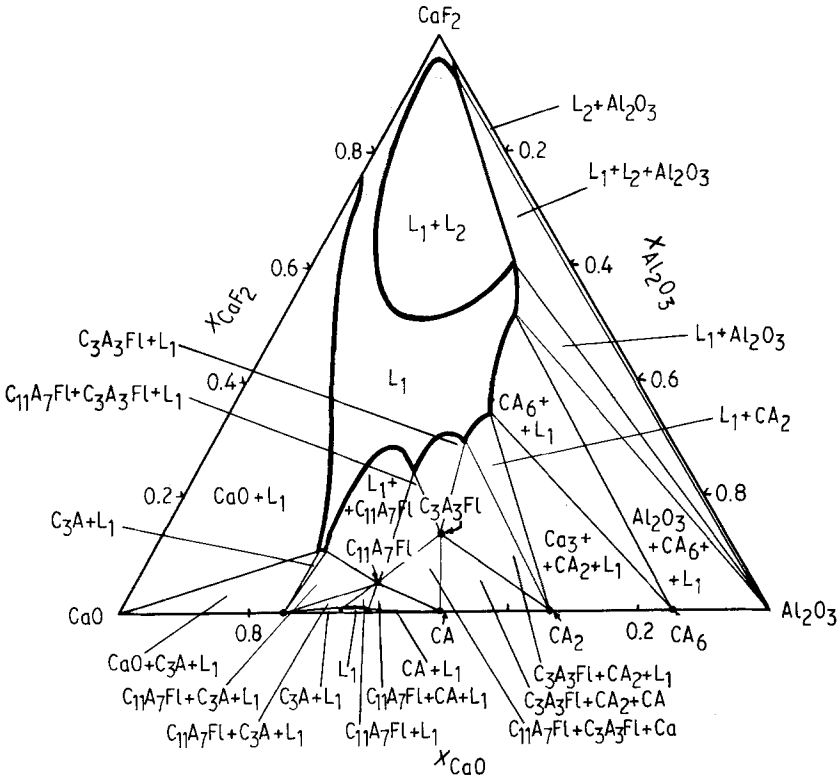

Figure 7 Computed isotherm at $T = 1723$ K for the CaF_2–Al_2O_3–CaO phase diagram.

be emphasized that the position of E_1 on the composition scale and its temperature have not been clarified experimentally [1] but obtained by extrapolation that leads inevitably to some uncertainties.

Point E_2 corresponds to final crystallization of the CA_6–CaF_2–Al_2O_3 triangle compositions. It has not been revealed in previous studies [1, 3]. This was the reason for a supposition that the peritectical beginning from the point of CA_6 peritectic decomposition passed through the CA_6–CaF_2 join and CaF_2–Al_2O_3 binary side, entered into the field of the CaF_2–Al_2O_3–AlF_3 triangle and ended in a ternary peritectic point. However, neither experimental nor theoretical confirmation of this concept were offered [1]. An experimental test of the concept is associated with some difficulties due to similarity of the CA_6 and Al_2O_3 optical characteristics and X-ray patterns [1]. In addition, it is difficult to maintain conditions that would exclude the exchange interaction $3CaF_2 + Al_2O_3 = 3CaO + 2AlF_3$ and CaO formation in the slag. Further, the suggestion [1] that the compound CA_6 are the first to precipitate in the

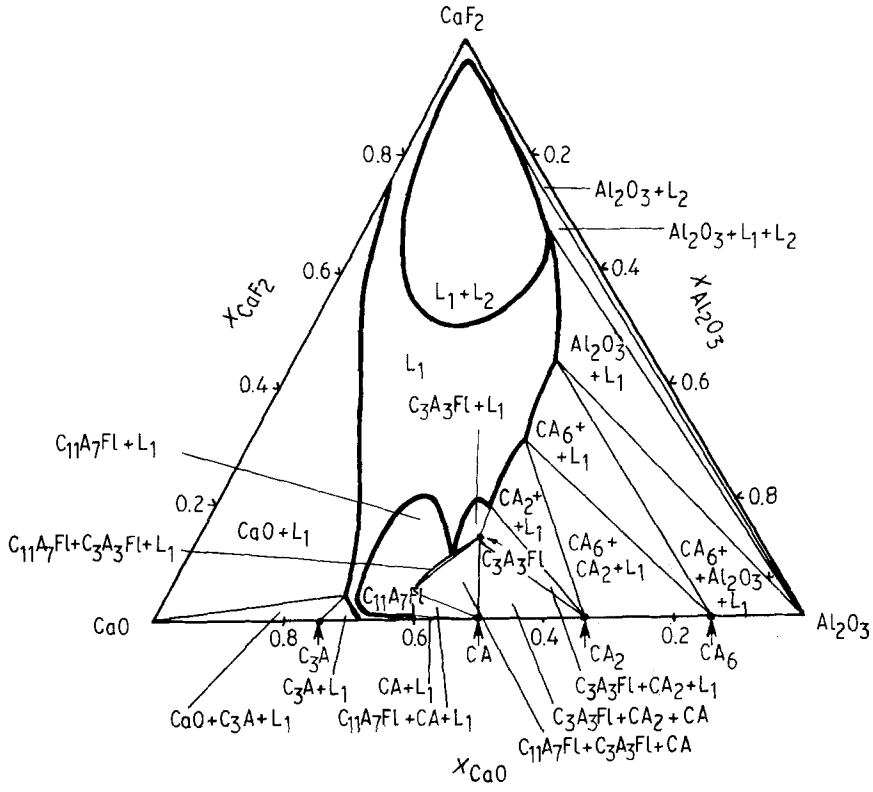

Figure 8 Computed isotherm at $T = 1773$ K for the CaF_2–Al_2O_3–CaO phase diagram.

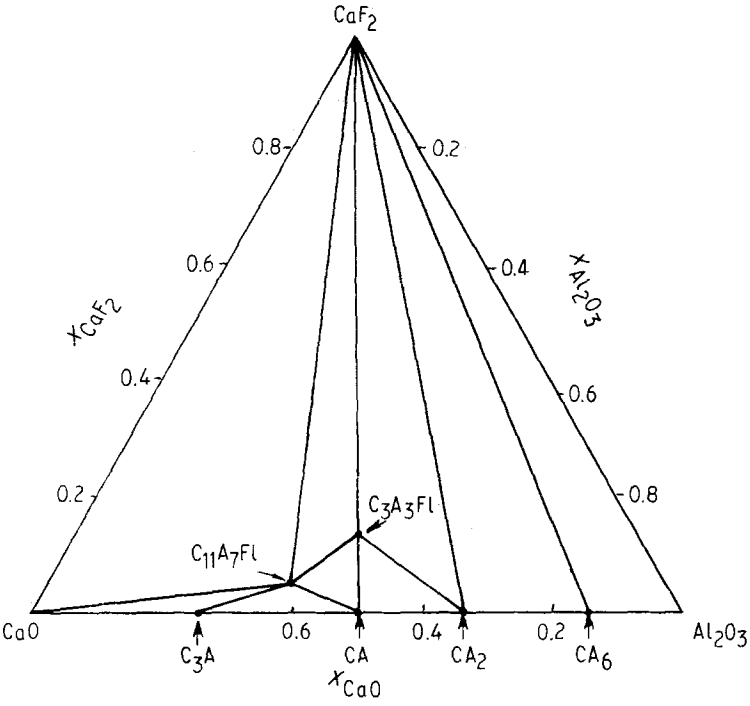

Figure 9 Triangulation of the CaF_2–Al_2O_3–CaO phase diagram.

CaF_2–Al_2O_3 junction does not seem reasonable because it decomposes into alumina and a liquid phase due to a peritectic reaction. The process scheme [1] suggested to explain residual CaO appearance in samples while studying the CaF_2–Al_2O_3 junction is contradictory. On the one hand, aluminium trifluoride formed by the exchange interaction is supposed to sublimate. On the other hand, it is evident that the AlF_3 concentration in the melt should be quite high for the liquid phase to correspond to a ternary peritectic point in the CaF_2–Al_2O_3–AlF_3 triangle.

The present calculations, based upon the experimentally found thermodynamic characteristics of all the phases of the CaF_2–Al_2O_3–CaO system, have shown that the peritectic line originates from the point of CA_6 peritectic decomposition and passes below the zone of liquid immiscibility, being one of its co-nodes, and ends in the ternary eutectic point E_2 of the CA_6–Al_2O_3–CaF_2 triangle. This conclusion agrees well with the experimental data of Izmailov [4], who detected a ternary eutectic point in the CaF_2–Al_2O_3–CaO triangle. The results of Raichenko and Litrinova [29] also contradict the data of Zhmoidin and Chatterjee [1]. The former authors [29] studied the influence of additions of calcium, magnesium and silicon oxides and temperature within the range 1273 to 1873 K upon the phase composition of

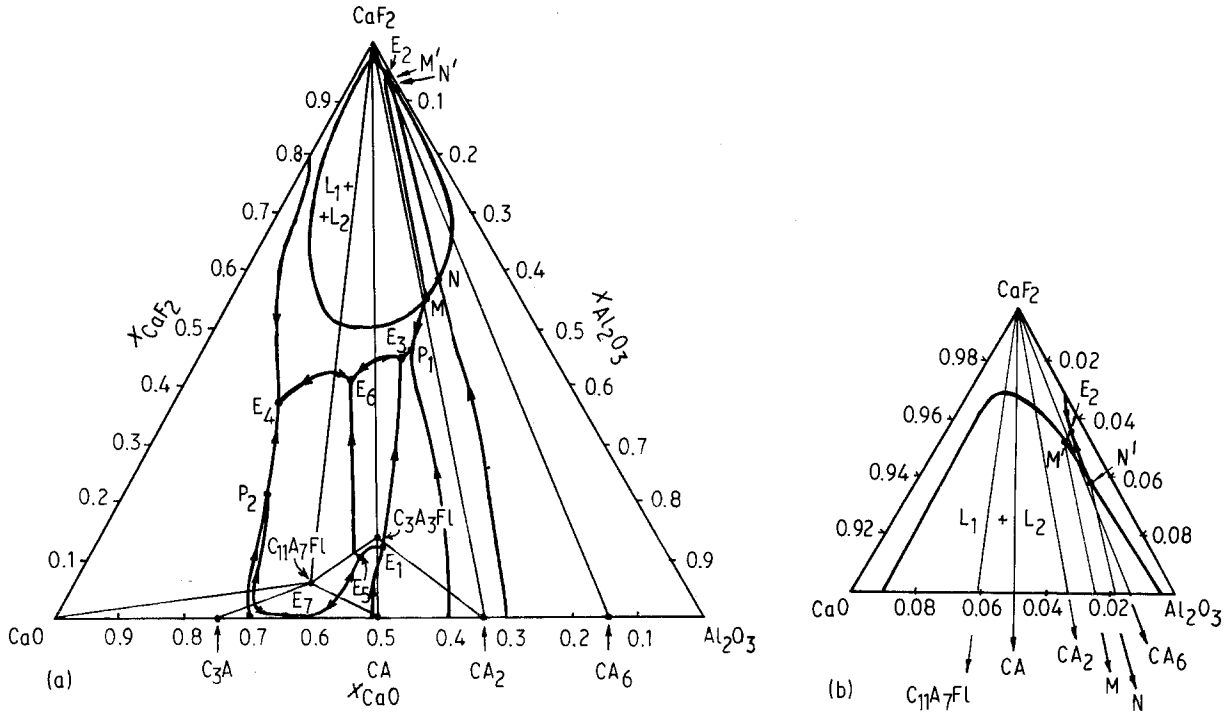

Figure 10 (a) Computed CaF_2–Al_2O_3–CaO phase diagram; (b) CaF_2 apex of the diagram.

TABLE I Invariant points of the CaF_2–Al_2O_3–CaO phase diagram according to the present investigation

Notation	Composition (mol %)		T(K)	Invariant equilibrium
	CaF_2	CaO		
E_1	12.9	43.3	1783	$L \rightarrow CA + CA_2 + C_3A_3Fl$
E_2	95.5	0.55	1667	$L \rightarrow CA_6 + CaF_2 + Al_2O_3$
E_3	45.1	23.2	1615	$L \rightarrow C_3A_3Fl + CA_2 + CaF_2$
E_4	37.8	46.4	1509	$L \rightarrow CaO + C_{11}A_7Fl + CaF_2$
E_5	11.5	47.3	1772	$L \rightarrow C_{11}A_7Fl + C_3A_3Fl + CA$
E_6	40.8	33.8	1606	$L \rightarrow C_{11}A_7Fl + C_3A_3Fl + CaF_2$
E_7	0.11	64.2	1623	$L \rightarrow C_{11}A_7Fl + CA + C_3A$
P_1	46.6	21.6	1623	$L + CA_6 \rightarrow CA_2 + CaF_2$
P_2	27.9	52.3	1597	$L + C_{11}A_7Fl + CaO \rightarrow C_3A$
M	55.6	14.3	1667	$L_{M'} \rightarrow L_M + CaF_2 + CA_6$
M′	95.3	0.68	1667	
N	58.1	11.1	1695	$L_N \rightarrow L_{N'} + CA_6 + Al_2O_3$
N′	93.8	0.81	1695	
C_3A_3Fl	14.28	42.86	1784	Congruent melting
$C_{11}A_7Fl$	5.26	57.90	1853	Congruent melting

TABLE II Invariant points of the CaF_2–Al_2O_3–CaO phase diagram according to the data of Zhmoidin and Chatterjee [1]

Notation	Composition (mol %)			T(K)	Invariant equilibrium
	CaF_2	Al_2O_3	CaO		
E'_1	8.2	47.7	44.1	< 1771	$L \rightarrow CA + CA_2 + C_3A_3Fl$
E'_2	~ 97.9	~ 1.5	~ 0.6	~ 1663	$L \rightarrow CA_2 + CA_6 + CaF_2$
E'_3	~ 96.8	~ 1.9	~ 1.3	~ 1658	$L \rightarrow C_3A_3Fl + CA_2 + CaF_2$
E'_4	36.45	15.35	48.2	1503	$L \rightarrow CaO + C_{11}A_7Fl + CaF_2$
E'_5	6.5	44.8	48.7	< 1748	$L \rightarrow C_{11}A_7Fl + C_3A_3Fl + CA$
P'_1	87.2	4.5	8.3	1628	$L + C_3A_3Fl \rightarrow C_{11}A_7Fl + CaF_2$
P'_2	1.2	29.0	69.8	1733	$L + CaO \rightarrow C_3A + C_{11}A_7Fl$
M_1	35.0	38.8	26.2	1745	$L_{M_1} \rightarrow L_{M'_1} + C_3A_3Fl + CA_2$
M'_1	94.8	3.1	2.1	1745	
N_1	50.8	37.2	12.0	1788	$L_{N_1} \rightarrow L_{N'_1} + CA_2 + CA_6$
N'_1	94.0	4.6	1.4	1788	
C_3A_3Fl	14.28	42.86	42.86	1780 ± 1.5	Congruent melting
$C_{11}A_7Fl$	5.26	36.84	57.90	1850 ± 2.5	Congruent melting

CaF_2–Al_2O_3 slags containing 70 wt % CaF_2 and 30 wt % Al_2O_3. They stated that alumina was the primary crystallizing phase, CA_6 being formed through the exchange reaction and its quantity raised as the time of exposure increased.

The present calculations have demonstrated that the ternary eutectic point found in the CA_2–CA_6–CaF_2 triangle by Zhmoidin and Chatterjee [1] is absent in reality. Final crystallization of slags belonging to this field of the phase diagram occurs at the peritectic point P_1 corresponding to the equilibrium $CA_6 + L \rightarrow CaF_2 + CA_2$. The lines of CA_6–CaF_2 binary crystallization lie below the field of the liquid miscibility gap, being one of the co-nodes. The final crystallization of slags of the C_3A_3Fl–CA_2–CaF_2 triangle takes place at the ternary eutectic point E_3. The position of E_3 is in the middle of the CaF_2–Al_2O_3–CaO phase diagram but not in the CaF_2-enriched part as suggested in other work [1, 2].

Point E_4 is the deepest ternary eutectic of the system under discussion. It corresponds to the process $L \rightarrow CaO + CaF_2 + C_{11}A_7Fl$. The coordinates found for E_4 (see Table I) are in a good agreement with the values obtained from experiments (Table II). In contrast to earlier conclusions [1, 2] the results of the calculations indicate that final crystallization of melts in the $C_{11}A_7Fl$–C_3A_3Fl–CaF_2 triangle occurs at the ternary eutectic point E_6 situated at $X_{CaF_2} = 0.408$, $X_{CaO} = 0.338$ and $T = 1606$ K. The earlier authors [1] believed that the latter process took place at $T = 1623$ K at a ternary peritectic point P_1' due to the transformation $L + C_3A_3Fl \rightarrow C_{11}A_7Fl + CaF_2$ (Table II). It should be emphasized that the temperatures of these two points E_6 and P_1 are near to each other. This nearness allows one to assume that the conclusion about the peritectic character of final crystallization of the $C_{11}A_7Fl$–C_3A_3Fl–CaF_2 triangle liquid is a result of the path of melt crystallization being incorrectly inferred [1]. The issue should be investigated further.

The final crystallization of slags with compositions belonging to the $C_{11}A_7Fl$–C_3A_3Fl–CA triangle takes place at the ternary eutectic point E_5. This fact is in good agreement with earlier results [1]. A comparison between the eutectic point coordinates (Tables I and II) does not mean anything because the eutectic position was determined by Zhmoidin and Chatterjee [1] from the course of conjunctive curves and has not been clarified by experiments.

The final crystallization of C_3A–$C_{11}A_7Fl$–CA triangle slags occurs at the ternary eutectic point E_7 situated in the neighbourhood of the eutectic point of the CaO–Al_2O_3 binary subsystem (Table I). This crystallization path of melts belonging to the above-mentioned field of the CaF_2–Al_2O_3–CaO phase diagram is established for the first time in the present study. The compound $C_{12}A_7$ has been supposed to exist in the C_3A–$C_{11}A_7Fl$–CA triangle in all preceding investigations. However, thermodynamic studies [21, 22, 27] and determination of the CaO–Al_2O_3 phase

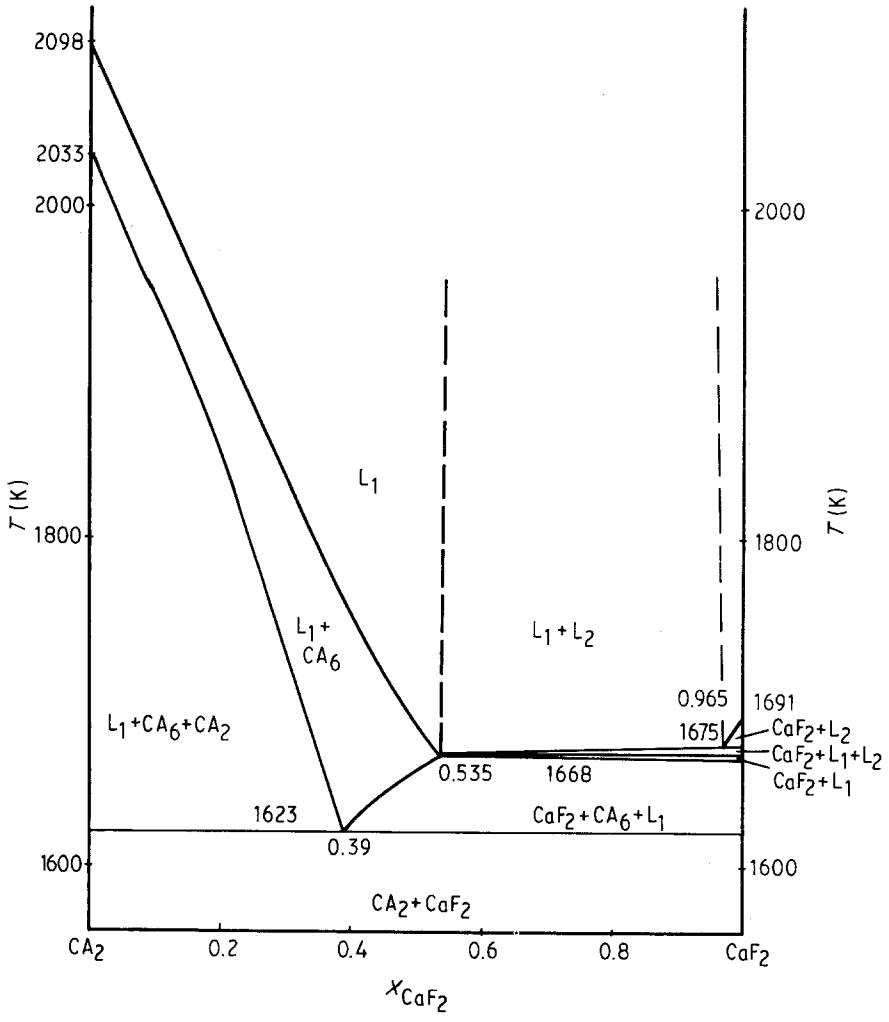

Figure 11 The computed junction CaF_2–CA_2 of the CaF_2–Al_2O_3–CaO phase diagram.

diagram under conditions excluding the penetration of moisture have shown the compound to be metastable, and therefore it should not be included in the $CaO–Al_2O_3$ phase diagram.

According to the calculations the peritectic point P_2 describing the final crystallization of the $CaO–C_{11}A_7Fl–C_3A$ triangle melts lies in the $CaO–C_{11}A_7Fl–CaF_2$ phase field but not $C_3A–C_{11}A_7Fl–CA$ in the region, as previously suggested [1, 2]. It corresponds to the process $L + CaO + C_{11}A_7Fl \rightarrow C_3A$.

There are two points of four-phase monotectic equilibrium M′ and N on the $CaF_2–Al_2O_3–CaO$ phase diagram. These points have been discussed earlier while considering crystallization of the slags belonging to $CA_6–CaF_2–Al_2O_3$ and $CA_2–CaF_2–CA_6$ triangles and we will not characterize them further. On the whole, the agreement between computed and experimentally found [1, 3] $CaF_2–Al_2O_3–CaO$ phase diagrams is quite satisfactory. It should be stressed that the computations based on experimentally found thermodynamic characteristics of all the phases in the system have allowed us to clarify a number of diagram details that were previously unknown, particularly in cases where experimental determination of the nature and composition of equilibrium phases were complicated by similarity of their optical properties, X-ray patterns and so on.

2.5. The $CaF_2–CA_2$ junction

To make the constitution of the $CaF_2–Al_2O_3–CaO$ phase diagram clearer, some of the joins are represented in Figs 11 to 17 below. The $CaF_2–CA_2$ join (Fig. 11) is not quasibinary. CaF_2 and CA_6 phases are the primary crystallizing ones. Complete crystallization of slags belonging to the junction under discussion takes place at the ternary peritectic point P_1 (see Fig. 10 and Table I). The liquid miscibility gap occupies a wide concentration region ranging from $X_{CaF_2} = 0.535$ to 0.957. Co-nodes of the immiscibility region do not lie in the plane of the $CaF_2–CA_2$ junction but their divergence in space is not appreciable. The slope of the base of the immiscibility region in the direction from the critical point toward the equilibrium line $L_{M'} \rightarrow L_M + CaF_2 + CA_6$ is slight, being equal to a few Kelvins. This is why the equilibrium fields of CaF_2 with L_1 and $L_1 + L_2$ are very narrow (Fig. 11) and occur within the temperature range 1668 to 1673 K. The CA_2 and CaF_2 phases are in a state of equilibrium after complete solidification of the liquid.

2.6. The $CA–CaF_2$ junction

The $CA–CaF_2$ junction (Fig. 12) is also not quasibinary. This fact is in contrast to the earlier conclusion [1]. A region of primary crystallization of calcium dialuminate is observed at the junctions. The positions

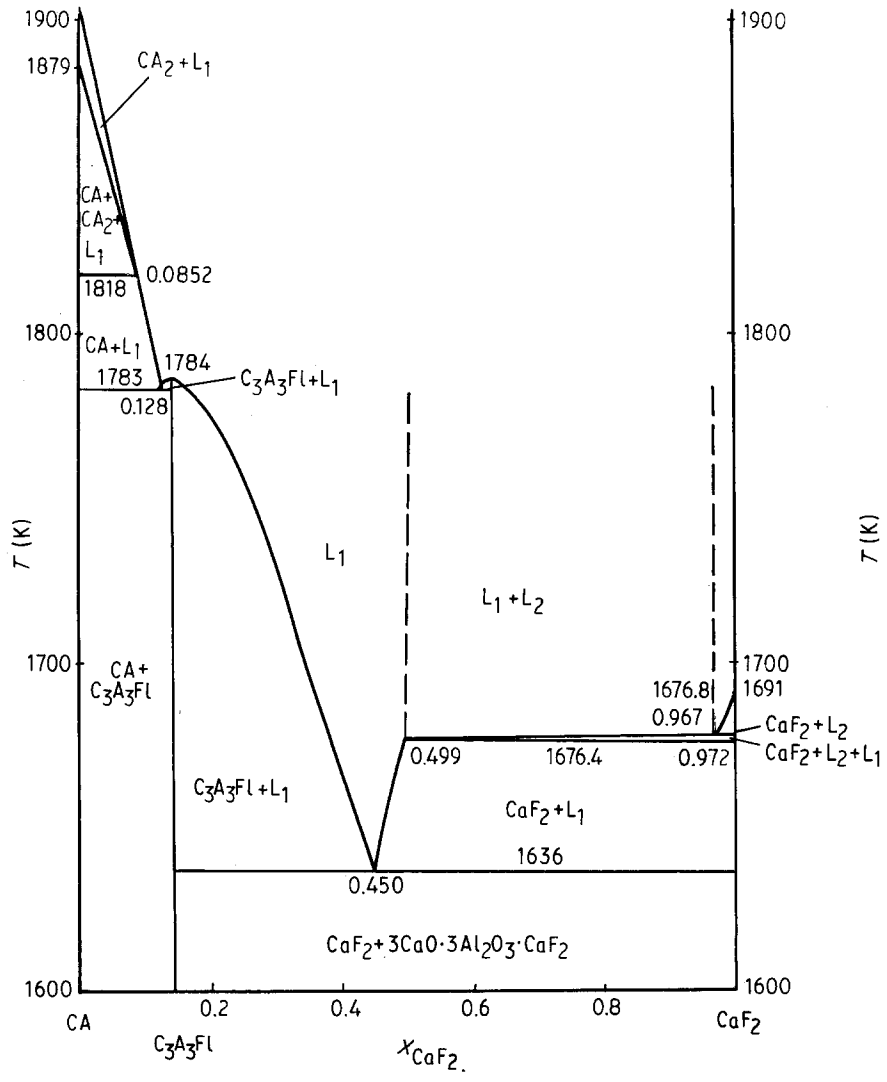

Figure 12 The computed junction $CA–CaF_2$ of the $CaF_2–Al_2O_3–CaO$ phase diagram.

of the co-nodes of the immiscibility zone do not coincide with the junction direction. However, because of the facts listed above the equilibrium field of CaF_2 with two liquids is very narrow (Fig. 12). There are two eutectic points at the join. The first one, with coordinates $X_{CaF_2} = 0.128$ and $T = 1783$ K, corresponds to the crystallization of slags with compositions between CA and C_3A_3Fl. The final solidification of slags belonging to the phase field between C_3A_3Fl and CaF_2 takes place at the second eutectic point with coordinates $X_{CaF_2} = 0.450$, $T = 1636$ K. The C_3A_3Fl compound melts congruently at $T = 1784$ K. It should be pointed out that in the case considered the equilibrium field of CaF_2 with L_1 is much wider than in the CA–CaF_2 junction.

2.7. The $C_{11}A_7Fl$–CaF_2 junctions

As the direction of the $C_{11}A_7Fl$–CaF_2 junctions does not coincide with the positions of co-nodes of the immiscibility zone, this cross-section (Fig. 13) may be interpreted as quasibinary but only conditionally. The equilibrium field $L_1 + L_2 + CaF_2$ is very narrow, as in the preceding cases. The slight slope of the immiscibility field base is confirmed by the practically full coincidence of the temperatures of separation into two

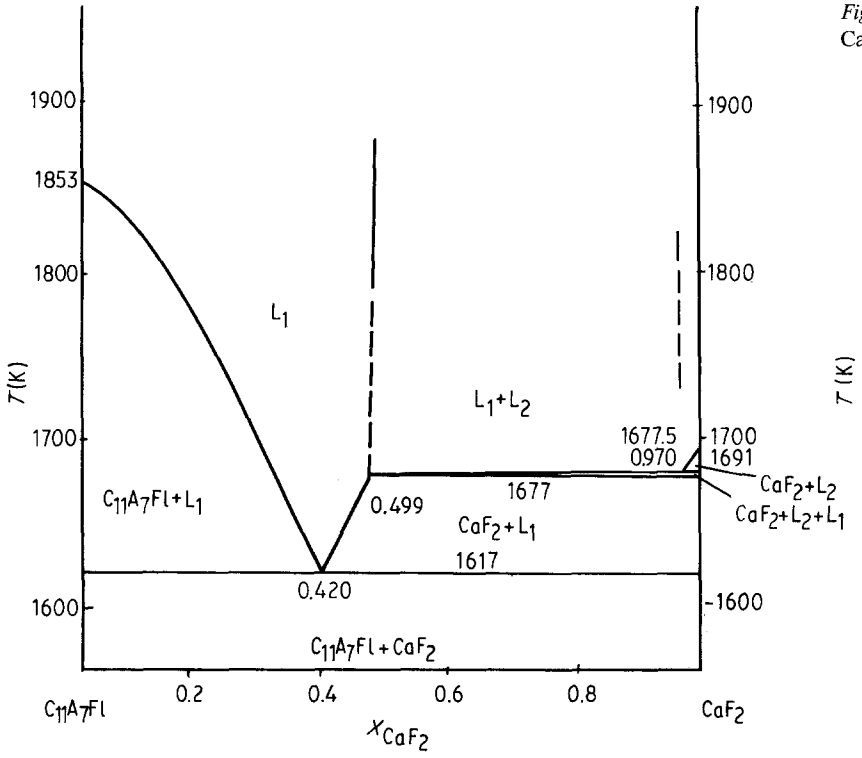

Figure 13 The computed junction $C_{11}A_7Fl$–CaF_2 of the CaF_2–Al_2O_3–CaO phase diagram.

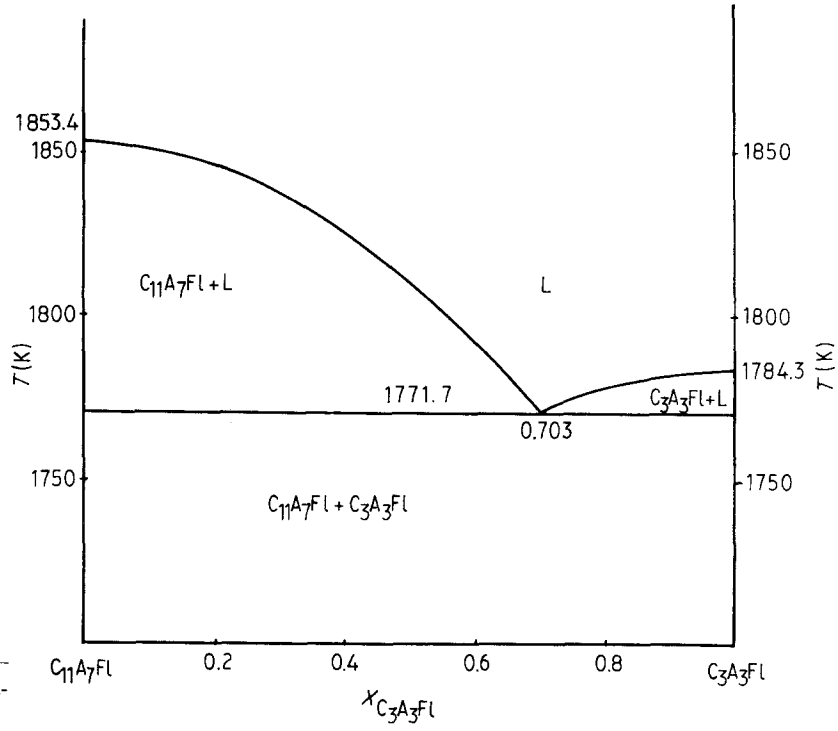

Figure 14 The computed junction $C_{11}A_7Fl$–C_3A_3Fl of the CaF_2–Al_2O_3–CaO phase diagram.

phases beginning at the CA–CaF_2 and $C_{11}A_7Fl$–CaF_2 junctions (1677 K, see Figs 12 and 13). The complete crystallization of the slag with compositions corresponding to the $C_{11}A_7Fl$–CaF_2 junction takes place at the eutectic point, the coordinates being $X_{CaF_2} = 0.420$ and $T = 1617$ K.

2.8. The junctions $C_{11}A_7Fl$–C_3A_3Fl, $C_{11}A_7Fl$–C_3A, $C_{11}A_7Fl$–CA and C_3A_3Fl–CA_2

The $C_{11}A_7Fl$–C_3A_3Fl junction (Fig. 14) was found to be quasibinary and like an ordinary eutectic phase diagram with the eutectic point located at $X_{C_3A_3Fl}$

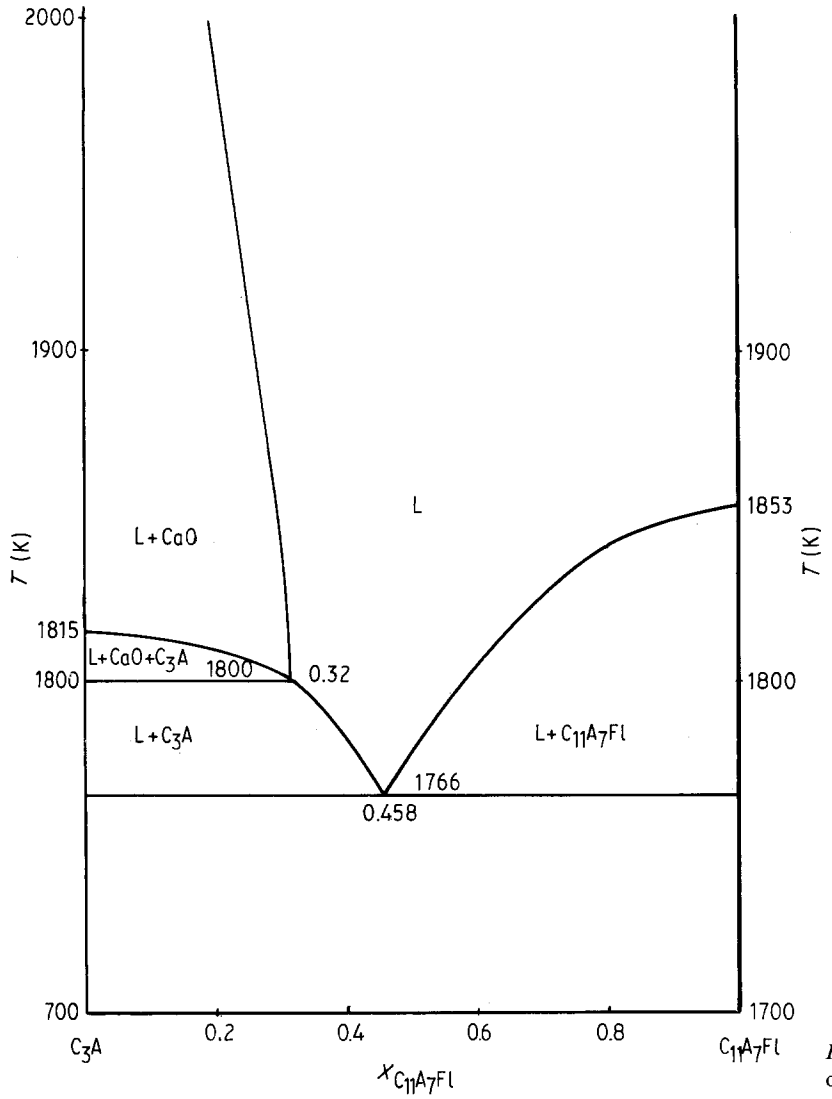

Figure 15 The computed junction $C_{11}A_7Fl$–C_3A of the CaF_2–Al_2O_3–CaO phase diagram.

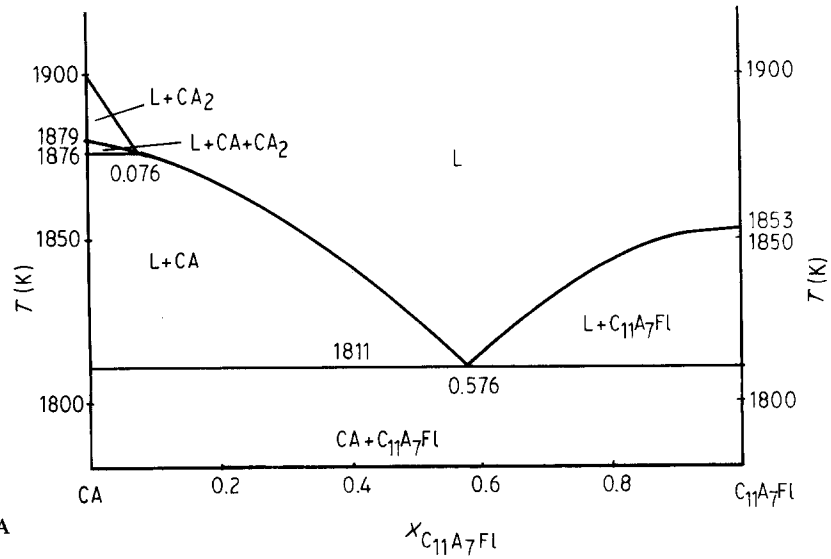

Figure 16 The computed junction $C_{11}A_7Fl$–CA of the CaF_2–Al_2O_3–CaO phase diagram.

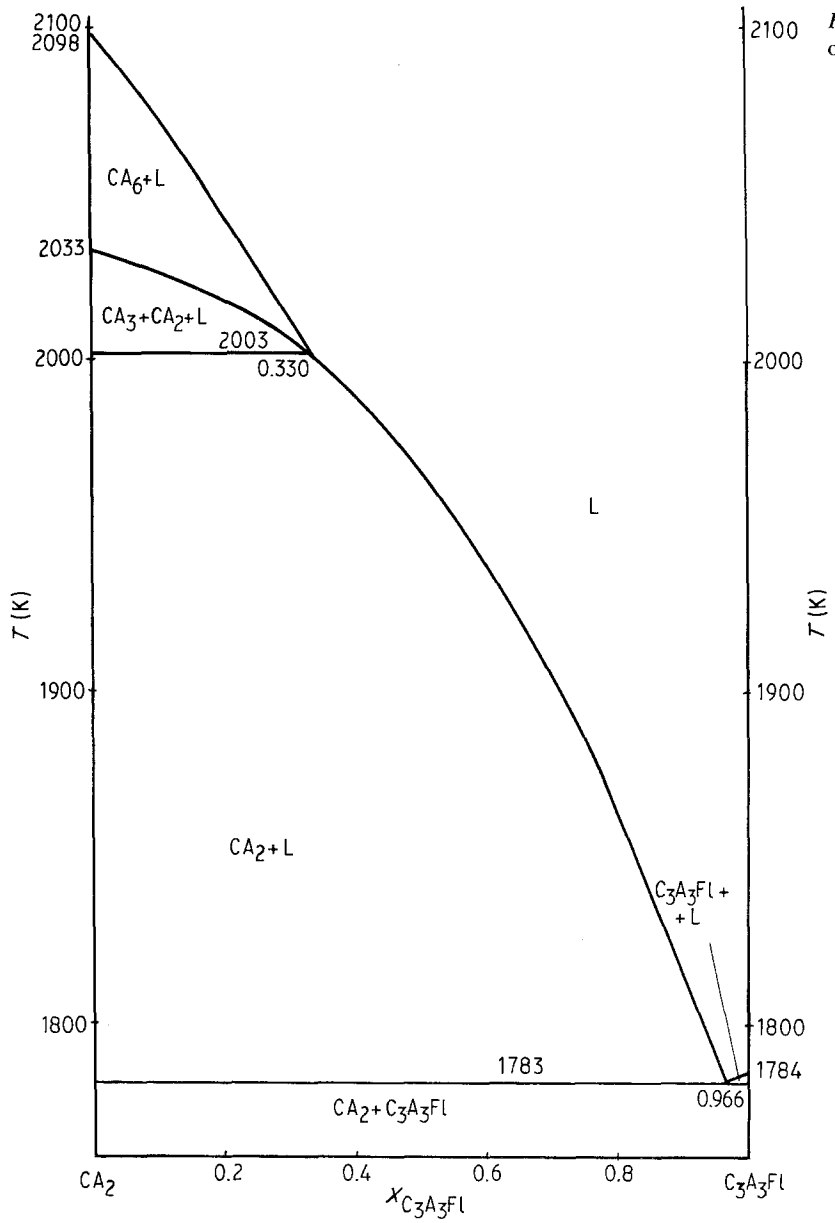

Figure 17 The computed junction C_3A_3Fl–CA_2 of the CaF_2–Al_2O_3–CaO phase diagram.

= 0.703 and $T = 1772$ K. Divergences of $C_{11}A_7Fl$–C_3A and $C_{11}A_7Fl$–CA junctions (Figs 15 and 16) from quasibinary ones are caused by incongruent melting of C_3A and CA. The $C_{11}A_7Fl$–C_3A junction has a wide region (up to $X_{C_{11}A_7Fl} = 0.32$ and $T = 1800$ K) of the primary field of CaO. The primary field of CA_2 in the $C_{11}A_7Fl$–CA junction (Fig. 16) is much narrower. The C_3A_3Fl–CA_2 junction has a similar constitution (Fig. 17). The primary field of CA_6 makes the join non-quasibinary. A eutectic point with the coordinates $X_{C_3A_3Fl} = 0.966$, $T = 1783$ K lies in this junction near to the compound C_3A_3Fl.

3. Summary

In conclusion it is necessary to underline that the present computation of phase equilibria was performed on the basis of thermodynamic functions obtained in experiments where the existence of thermodynamic equilibria had been proved [21–24]. More than that, coordinates of a number of points on phase equilibrium boundaries were found in experiments on isothermal evaporation of slags. Data obtained in this way agree excellently with the results of the computations. The latter fact, as well as the agreement with the majority of information available as discussed above, prove the reliability of the results derived in the present study. The computations accomplished allowed us to reveal a set of details and peculiarities of the constitution of the CaF_2–Al_2O_3–CaO phase diagram.

Acknowledgements

The authors would like to express their deep gratitude to M. A. Zemchenko and E. A. Gaidash for assistance in the preparation of the paper.

References

1. G. I. ZHMOIDIN and A. K. CHATTERJEE, "Slags for Metal Refining. Properties Variations of System CaO–Al_2O_3–CaF_2" (Metallugiya, Moscow, 1986) p. 286.
2. K. C. MILLS and B. J. KEENE, *Int. Met. Rev.* **1** (1981) 21.
3. R. RIES and K. SCHWERDTFEGER, *Arch. Eisenh-ü-ttenw.* **51** (1980) 123.
4. Yu. G. IZMAILOV, "Issledovaniye sistemy CaO–Al_2O_3–CaF_2 v usloviyakh ispareniya ftoristykh soedinenii", Avtoref. kand. diss., Chelyabinsk (1976).

5. D. Ya. POVOLOTSKII, G. P. VYATKIN and Yu. G. IZMAILOV, *Sb. Nauch. Trudov Chelyabinsk. Politekhn. Inst. No.* 166 (1975) 35.
6. R. NAFZIGER, *High Temp. Sci.* **5** (1974) 414.
7. A. K. CHATTERJEE and G. I. ZHMOIDIN, *J. Mater. Sci.* **7** (1972) 93.
8. G. S. SMIRNOV, A. K. CHATTERJEE and G. I. ZHMOIDIN, *ibid.* **8** (1973) 1278.
9. W. GUTT, A. K. CHATTERJEE and G. I. ZHMOIDIN, *ibid.* **5** (1970) 960.
10. A. K. CHATTERJEE and G. I. ZHMOIDIN, *Izv. Akad. Nauk SSSR, Neorg. Mater.* **10** (1974) 1846.
11. *Idem, ibid.* **8** (1972) 883.
12. G. I. ZHMOIDIN and A. K. CHATTERJEE, *Izv. Akad. Nauk SSSR, Metally No.* 6 (1971) 46.
13. A. K. CHATTERJEE, T. Ya. MALYSHEVA and G. I. ZHMOIDIN, *ibid. No.* 6 (1970) 58.
14. L. H. HILLERT, *Acta Polytechn. Scand.* **90** (1970) 115.
15. G. I. ZHMOIDIN, *Izv. Akad. Nauk, Metally No.* 6 (1969) 9.
16. M. W. DAVIES and F. A. WRIGHT, *Chem. Industry* (1970) 359.
17. G. J. W. KOR and F. D. RICHARDSON, *Trans. AIME* **245** (1969) 319.
18. D. M. EDMUNDS and J. TAYLOR, *J. Iron. Steel Inst.* **210** (1972) 280.
19. M. ALLIBERT, J. F. WADIER and A. MITCHELL, *Ironmaking Steelmaking* **5** (1978) 211.
20. P. P. EVSEEV, L. I. SINYUKOVA and A. F. FILLIPOV, *Izv. Vuzov, Chernaya Metallurgiya* **1** (1966) 74.
21. A. I. ZAITSEV, N. V. KOROLYOV and B. M. MOGUTNOV, *Z. Fiz. Khim.* **64** (1990) 1494.
22. *Idem, ibid.* **64** (1990) 1505.
23. *Idem, J. Chem. Thermod.* **22** (1990) 513.
24. *Idem, ibid.* **22** (1990) 531.
25. P. PASCAL, *Z. Elektrochem.* **19** (1913) 610.
26. R. W. NURSE, J. H. WELCH and A. J. MAJUMDAR, *Trans. Br. Ceram. Soc.* **64** (1965) 409.
27. R. V. KUMAR and D. A. R. KAY, *Met. Trans.* **16B** (1985) 107.
28. A. I. ZAITSEV, N. V. KOROLYOV and B. M. MOGUTNOV, *Akad. Nauk. SSSR, Rasplavy* **3** (1989) 58.
29. T. F. RAICHENKO and T. I. LITVINOVA, *Izv. Akad. Nauk, Metally No.* 4 (1971) 105.

Received 20 June
and accepted 22 November 1989